TU Delft

Delft University of Technology

Investigating polarization effects of CO_2 adsorption in MgMOF-74

Becker, TM; Dubbeldam, D; Lin, Li-Chiang; Vlugt, TJH

DOI
10.1016/j.jocs.2015.08.010

Publication date
2016

Document Version
Final published version

Published in
Journal of Computational Science

Citation (APA)
Becker, TM., Dubbeldam, D., Lin, L.-C., & Vlugt, TJH. (2016). Investigating polarization effects of CO_2 adsorption in MgMOF-74. *Journal of Computational Science*, *15*, 86-94. https://doi.org/10.1016/j.jocs.2015.08.010

Important note
To cite this publication, please use the final published version (if applicable).
Please check the document version above.

Copyright
Other than for strictly personal use, it is not permitted to download, forward or distribute the text or part of it, without the consent of the author(s) and/or copyright holder(s), unless the work is under an open content license such as Creative Commons.

Takedown policy
Please contact us and provide details if you believe this document breaches copyrights.
We will remove access to the work immediately and investigate your claim.

This work is downloaded from Delft University of Technology.
For technical reasons the number of authors shown on this cover page is limited to a maximum of 10.

Journal of Computational Science 15 (2016) 86–94

Contents lists available at ScienceDirect

Journal of Computational Science

journal homepage: www.elsevier.com/locate/jocs

Investigating polarization effects of CO_2 adsorption in MgMOF-74

Tim M. Becker[a], David Dubbeldam[b], Li-Chiang Lin[a], Thijs J.H. Vlugt[a,*]

[a] Engineering Thermodynamics, Process & Energy Department, Faculty of Mechanical, Maritime and Materials Engineering, Delft University of Technology, Leeghwaterstraat 39, 2628CB Delft, The Netherlands
[b] Van 't Hoff Institute for Molecular Sciences, University of Amsterdam, Science Park 904, 1098XH Amsterdam, The Netherlands

ARTICLE INFO

Article history:
Received 6 May 2015
Received in revised form 22 July 2015
Accepted 30 August 2015
Available online 2 September 2015

Keywords:
Polarization
Force field
Carbon capture
MgMOF-74
Monte Carlo simulation

ABSTRACT

MgMOF-74 is a promising candidate for a variety of gas separation applications, e.g., carbon capture and natural gas sweetening due to its high CO_2 uptake capacity and its favorable selectivity toward CO_2. Motivated by its promising properties, MgMOF-74 has been extensively studied both experimentally and computationally. Experimentally determined adsorption isotherms show an inflection at a loading of approximately one CO_2 molecule per magnesium ion due to strong adsorption sites close to the ions. It is a great challenge to accurately reproduce this behavior in molecular simulations. In this study, we explicitly consider polarization between the adsorbed CO_2 molecules and the framework of MgMOF-74 via the induced point dipole method. Back-polarization is neglected to achieve reasonable simulation times. To account for implicitly incorporated polarization, we rescale the Lennard–Jones energy parameters with respect to the atomic polarizabilities. A series of Monte Carlo simulations of CO_2 in MgMOF-74 is conducted. The computed CO_2 adsorption isotherm is in good agreement with experimental measurements and previous simulation results using a DFT-derived force field. This indicates that polarization is important for describing the adsorption of CO_2 in MgMOF-74. The direct inclusion of polarization will lead to force fields with better physical justification and transferability.

© 2015 Elsevier B.V. All rights reserved.

1. Introduction

The acceleration of climate change is one of the big challenges modern society is facing [1]. One of the major causes is the enormous amount of carbon dioxide emitted by power plants, especially coal-fired power plants [2]. Carbon capture and sequestration is a viable near-term solution to mitigate this development [3,4]. A promising technology in this context is to separate the CO_2 from the flue gas via solid adsorbents [5]. In particular, Metal-Organic Frameworks (MOFs) have been shown to provide opportunities for this application [4]. The amount of theoretically possible MOF structures is almost unlimited [6]. Many of these structures have exceptionally large surface areas and the geometry of the cavities can be chosen according to a specific application [7]. MgMOF-74 is of special interest for carbon capture because of its high CO_2 uptake capacity and its favorable selectivity toward carbon dioxide over nitrogen, even in the low pressure region relevant to carbon capture [8]. The framework of MgMOF-74 consists of one-dimensional hexagonal pores with a diameter between 11 and 12 Å[9]. Coordinatively unsaturated magnesium ions are embedded into this framework. The strong affinity of MgMOF-74 toward CO_2 arises from interactions with the so-called "open metal" sites [10]. MgMOF-74 has been extensively studied both experimentally [11,9] and computationally [12–15]. In experiments, an inflection at a loading of approximately one CO_2 molecule per open metal site is observed, and this behavior is associated with the saturation of the open metal sites and the subsequent filling of the less favorable centers of the pores [10]. It is a major challenge to quantitatively predict the inflection and the shape of the adsorption isotherm using molecular simulation. Recently, several computational studies have been performed to model such a system [14,16,15]. These studies used rather simplified interaction models for guest–host interactions (Buckingham or Lennard–Jones potentials and electrostatic interactions with static partial charges without explicitly accounting for the polarization effect close to the open metal sites). However, polarization has been observed [17] and it has been suggested to contribute to the enhanced CO_2 affinity in MgMOF-74 [18]. Our approach is to consider polarization explicitly with a polarizable force field and to compute the CO_2 uptake in grand-canonical Monte Carlo simulations. Polarizable force fields are frequently used in Molecular Dynamics simulations, e.g., for biological systems [19–21]. However, they are rarely applied in

* Corresponding author.
E-mail address: t.j.h.vlugt@tudelft.nl (T.J.H. Vlugt).

http://dx.doi.org/10.1016/j.jocs.2015.08.010
1877-7503/© 2015 Elsevier B.V. All rights reserved.

Monte Carlo simulations especially for guest molecules in solid adsorbents. The reason for this is that in principle, a computationally expensive method is required for every Monte Carlo step [22]. To the best of our knowledge, we are the first to apply a polarizable force field in a Monte Carlo simulation of a MOF with open metal sites. We apply the induced point dipole method to account for polarization additional to repulsion and dispersion interactions with a standard Lennard–Jones interaction potential. To achieve reasonable simulation times, back-polarization is neglected in our simulations. In standard force fields averaged polarization is implicitly accounted for. This contribution needs to be removed from the force field before polarization can be added explicitly. This is regarded for by adjusting the Lennard–Jones energy parameters deployed without polarization. We follow a simple procedure to rescale the Lennard–Jones energy parameters with respect to the assigned atomic polarizabilities. We herein demonstrate that the computed CO_2 adsorption isotherms using the polarizable force field approach are in good agreement with both experimental measurements and previously proposed force fields derived from quantum mechanical calculations, indicating polarization has a crucial role to play. The consideration of polarization in Monte Carlo simulations is also promising for other systems in which polarization is clearly not negligible [19,23], i.e., water [20], simulations including ions [19,24], or xylenes [25]. It may lead to more sophisticated force fields and to more physical models with better transferability.

In this study, we provide a brief overview of non-bonded intermolecular interactions and on how to account for induction interactions in molecular simulations. We motivate the necessity of adjusting the potential parameters taken from standard force fields according to the induction interactions (Section 2). The simulation details are provided in Section 3. We illustrate the procedure on the example of CO_2 adsorption in MgMOF-74 and compare the results to simulations with a generic force field and a force field deducted from density functional theory (DFT) [15] (Section 4). Our findings are summarized in Section 5.

2. Intermolecular interactions

An essential component of each molecular simulation is the description of the interactions between atoms and molecules. In general, the contributing interactions arise in some way from the electrostatic interactions between the charge distributions of molecules [26]. Most accurately, these interactions can be computed by quantum mechanical calculations. Unfortunately, these calculations are currently too time consuming to be applied in molecular simulations for large systems. Hence, potential functions are used to describe the interaction energy between atoms and molecules as a function of their positions. Due to increasing computing power, hybrid molecular and quantum mechanical simulations have become feasible for systems with moderate size [27]. In this work, we focus on interactions classically considered in molecular simulations between non-bonded particles that are not involved in chemical reactions. The level of detail and the type of interactions necessary in the simulations depends on the specific system and on the required accuracy of the predictions. To investigate structure-property relations or to screen materials for a certain application, generic force fields like UFF [28] or DREIDING [29] are often chosen. In these cases, the computation time is a crucial factor [27]. To make more accurate predictions, it is often required to deploy interaction potentials that are especially designed to reproduce the behavior of a particular system [27,30].

Molecular interactions are often divided into short and long range interactions with respect to how fast they decay with the distance between interacting particles. At very small interatomic distances, the electron clouds of atoms overlap, and a strong repulsive interaction arises that determines how close two atoms or molecules can ultimately approach each other. These repulsive interactions are sometimes referred to as exchange repulsion, hard core repulsion, steric repulsion, or, for ions, the Born repulsion. Strictly speaking, repulsive interactions belong to the category of quantum mechanical or chemical forces, and unfortunately there is no general equation for describing their distance dependence. Instead, a number of empirical potential functions have been introduced, all of which appear to be reasonable as long as they have the property of a steeply rising repulsion at small separations. The three most commonly used potentials for describing these interactions are the hard sphere potential, the inverse power-law potential, and the exponential potential [31].

Electrostatic interactions describe Coulombic interaction between charge densities of molecules. In comparison to other interactions, their strength decays slowly with the distance between molecules. This long-range behavior makes the computation more expensive and several methods to compute electrostatic interactions have been proposed, e.g., the Ewald summation technique [32] and its variants like Particle Mesh Ewald [33]. The Wolf method [34,35] is a computationally less expensive alternative for the Ewald summation. In molecular simulations, electrostatic interactions are usually considered through static partial charges assigned to interaction sites. Higher order multipole interactions can be modeled depending on how the interaction sites are distributed along the molecules. A precise representation requires specification of all non-zero multipole moments. Electrostatic interactions are strictly pairwise additive, highly anisotropic and can be either repulsive or attractive [36].

Dispersion interactions are significant to the total interactions and present for all systems. They play a role in a host of important phenomena such as adhesion, surface tension, physical adsorption, wetting, the properties of gases, liquids, and thin films, the strengths of solids, the flocculation of particles in liquids, and the structures of condensed macro molecules such as proteins and polymers [37–40]. Dispersion interactions are quantum mechanical in origin. They arise from correlated fluctuations between the motion of electrons. These fluctuations result in a lowering of the energy [26]. Thus, dispersion interactions are attractive. Numerically, dispersion interactions at long ranges can be described by a series in intermolecular separation r [27]. The leading term is power of $1/r^6$, while higher order terms are usually neglected in molecular simulations for computational simplicity [27]. The strength of the dispersion interactions depends on the number of electrons in the outer shell of an atom [41].

Induction interactions result from a distortion of the electron density of a molecule due to an electric field [20], e.g., caused by the charge distribution of another molecule. The difference in the electron density can be captured by adjusted multipole moments. Polarization can induce multipole moments even for spherical particles without static multipole moments [36]. Every change in the electron density again causes an alteration of the electric field. Consequently, the induction of a system depends on the interactions of the induced and static multipole moments of all molecules in the system. This dependency results in non-additivity and cannot be treated as a sum of pairwise additive atom–atom interactions [20]. For some systems, the effect of induction is small and it can be neglected [41]. If this contribution is large, the simplest solution in molecular simulations is modifying the static properties of each molecule to enhance the average interactions. However, this approach results in force fields with poor transferability and it is seldom suitable for systems with highly polarizable molecules like water or for biological systems like proteins or lipids [19].

The most commonly used interaction potential to describe molecular interactions in molecular simulations is the Lennard–Jones potential:

$$U_{\mathrm{LJ}}(r) = 4\varepsilon \left[\left(\frac{\sigma}{r}\right)^{12} - \left(\frac{\sigma}{r}\right)^{6} \right], \tag{1}$$

where ε characterizes the energy, σ is the distance scale of the atom or molecule interactions, and r is the interatomic distance. The $1/r^{12}$ term approximates the behavior of the repulsion energy and the $1/r^6$ term represents the behavior of the dispersion energy as a function of the distance between particles. Static charge distributions can be represented as static partial charges and are usually computed via the Ewald summation technique. To reproduce experimental results the potential parameters and static partial charges are often fitted to experimental data [42,43]. For instance, the TraPPE force fields for carbon dioxide and nitrogen are calibrated to reproduce vapor–liquid equilibria of the pure components and their mixtures with alkanes [30]. The resulting potential parameters of the Lennard–Jones potential and the static partial charges are effective values, since all occurring interactions are indirectly included in the parametrization. Another approach is to derive the potential parameters from quantum mechanical calculations [16,14,15]. Carefully calibrated Lennard–Jones models are usually quite satisfactory and are therefore popular [32,44]. The model captures the first order effects, but as the fitted parameters are adjustable parameters, also a large portion of the remaining physics is effectively incorporated [20,19]. As a result, the effective Lennard–Jones potential parameters may not be transferable between diverse molecular systems. The dependency of the charge distribution on the physical state of the system, composition and the fluctuations of the electric field caused by molecular motion can never be fully captured. An effective interaction potential calibrated in an environment of weak polarizability will most likely fail in a highly polarizable system, because it predicts the interaction strength incorrectly. This becomes crucial if polarization effects are strongly localized in the system, e.g., for biomolecular systems, like lipid-bilayers [19] or proteins [20,45,23]. In this case, it is inevitable to apply a force field that incorporates this phenomena. Unfortunately, the inclusion of polarization increases the computational costs significantly in Monte Carlo simulations. The effect of polarization has to be evaluated for every interaction site in every simulation step. Due to increasing computational power, now it becomes more feasible to include explicit polarization in molecular simulations [20].

The three most common methods to incorporate polarization in molecular simulations are the fluctuating charge method, the shell model, and the induced point dipole method [21,46–49]. These methods are additional to the interaction potentials normally applied in molecular simulations (e.g., Lennard–Jones potential and Coulombic interactions with static partial charges).

The fluctuating charge method allows the values of the partial charges assigned to interaction sites to change as a respond to the electric field. Hence, the charges are treated as dynamic properties. Charges can be transferred between interaction sites of a single molecule or even between separated molecules. The electronegativities and chemical hardnesses determine how easily charges can be exchanged from one interaction site to another. For every simulation step, or Monte Carlo trial move, instantaneous values of the partial charges are determined by minimizing the electrostatic energy of the system. In this approach, all order multipoles are considered and no new interactions need to be introduced. The drawback of the method is an artificial restriction of the direction of the polarization depending on the molecular shape [19,20], e.g., a linear and rigid representation of a molecular can only transfer charges in the direction of its extent.

In the shell model, explicit induced dipole interactions are considered and higher order induced multipole moments are neglected. Polarizable sites are described via a pair of charges. One charge is assigned to the nucleus while the other charge is connected to it by a harmonic spring. The values of the charges are kept fixed during the simulation and polarization is obtained via the relative displacement caused by electric interactions with the system. Consequently, there is no charge transfer between molecules. In this method, interactions between the charges of one polarizable site are not calculated. The magnitude of the charges and the value of the spring constant can be related to the polarizability, but they are often treated as tunable variables of the model. The computational costs increase due to the doubling of the electrostatic interaction sites and the requirement of smaller time steps in MD simulations. The reduction of the time step size is a necessity because of the division of the atomic mass between the nucleus and the shell charge. Thereby, the mass of the shell charge needs to be small in comparison to the nucleus to enable a rapid respond of its position to the electric field. Accordingly, the size of the time step has to be decreased due to smaller occurring masses [19,20,50].

In the induced point dipole method, isotropic dipole–dipole polarizabilities α_i are assigned to interaction sites i. Higher order multipole moments are neglected. Induced dipoles can be calculated for every interaction site as the result of the electrostatic field $\mathbf{E}_i$. Assuming a linear response for a single isolated point dipole, the induced dipole moment $\boldsymbol{\mu}_i$ can be determined via [20]:

$$\boldsymbol{\mu}_i = \alpha_i \cdot \mathbf{E}_i. \tag{2}$$

The electric field $\mathbf{E}_i$ is a function of the permanent electric field $\mathbf{E}_i^0$ caused by the static partial charges, and the induced dipoles of all N interaction sites in the system:

$$\mathbf{E}_i = \mathbf{E}_i^0 - \sum_{j \neq i} \mathbf{T}_{ij} \cdot \boldsymbol{\mu}_j, \tag{3}$$

where $\mathbf{T}_{ij}$ is the dipole field tensor:

$$\mathbf{T}_{ij} = \frac{1}{r^3}\mathbf{I} - \frac{3}{r^5} \begin{pmatrix} x^2 & xy & xz \\ yx & y^2 & yz \\ zx & zy & z^2 \end{pmatrix}. \tag{4}$$

Here, $\mathbf{I}$ is the identity matrix, x ($=x_i - x_j$), y ($=y_i - y_j$), z ($=z_i - z_j$) and r are respectively the components and the length of the vector between interaction sites i and j. In the induced point dipole method, the energy of the induced dipoles U_{ind} has three contributions:

$$U_{\mathrm{ind}} = U_{\mathrm{stat}} + U_{\mu\mu} + U_{\mathrm{pol}}. \tag{5}$$

U_{stat} is the interaction energy between the permanent electric field and the induced dipoles:

$$U_{\mathrm{stat}} = -\sum_{i=1}^{N} \boldsymbol{\mu}_i \cdot \mathbf{E}_i^0. \tag{6}$$

The energy $U_{\mu\mu}$ results from the interactions among the induced dipoles:

$$U_{\mu\mu} = \frac{1}{2}\sum_{i=1}^{N}\sum_{j \neq i} \boldsymbol{\mu}_i \cdot \mathbf{T}_{ij} \cdot \boldsymbol{\mu}_j. \tag{7}$$

The final energy contribution is the polarization energy U_{pol}, which describes the energy necessary to create the induced dipoles by changing the electron distribution:

$$U_{\mathrm{pol}} = \frac{1}{2}\sum_{i=1}^{N} \boldsymbol{\mu}_i \cdot \mathbf{E}_i. \tag{8}$$

By inserting Eqs. (6)–(8) into Eq. (5) and using Eq. (3) to replace $\mathbf{E}_i$, the relation for U_{ind} reduces to:

$$U_{\text{ind}} = -\frac{1}{2}\sum_{i=1}^{N} \boldsymbol{\mu}_i \cdot \mathbf{E}_i^0. \tag{9}$$

To solve Eq. (9) and to compute the induction energy, different techniques have been suggested, i.e., matrix inversion, the extended Lagrangian method, and iteration. The matrix inversion approach is to solve the dependent equations of all N induced dipole moments $\boldsymbol{\mu}_i$ (Eqs. 2 and 3) simultaneously by forming a matrix, inverting it and subsequently solving Eq. (9). However, for N polarizable interaction sites this involves inverting a $N \times N$ matrix at every simulation step. Due to the high computational time of matrix inversions this procedure is not feasible for medium-to-large systems [20]. An alternative approach is to use the extended Lagrangian method. In this approach, each dipole moment is treated as a dynamic quantity with its own mass. Thus, the dipoles follow their own equation of motion in the same way as the atomic positions. The assigned masses have no physical meaning, though they determine the efficiency and accuracy of the simulation [20]. The Lagrangian method is well suited for molecular dynamic simulations, but it is more complicated in Monte Carlo simulations. New Monte Carlo trial moves changing the dipoles were previously designed to tackle this problem [22]. Another approach is to iterate Eq. (2) to self-consistency. Typically, this requires between 2 and 10 iterations [20]. A possible initial guess for the electric field is the electric field created by the static charges [20]. This approach can be implemented in a Monte Carlo algorithm without any additional moves.

3. Simulation details

Monte Carlo simulations in the grand-canonical ensemble are conducted to compute the uptake of CO_2 in MgMOF-74 for varying pressures of the surrounding gas phase. The simulations were performed using the RASPA software package [51–53]. The atomic structure of MgMOF-74 is DFT-based and taken from Dzubak et al. [14]. The Lennard–Jones potential is truncated at a cutoff distance of 12.8 Å. No tail correction is applied. Periodic boundary conditions are used, and the simulation box is composed of multiple unit cells to ensure a distance of at least twice the cutoff radius between periodic images. To calculate electrostatic interactions between static partial charges the Ewald summation technique is used. Polarization is considered via the induced point dipole method [20]. We chose the procedure of Lachet et al. [25]. A schematic description of the procedure is shown in Fig. 1. The procedure avoids the iterative computation of the electric field, the so-called back-polarization. Thereby, reasonable simulation times can be achieved. To further reduce the simulation time, we use trivial parallelization, i.e., running several simulations concurrently and subsequently averaging over the results to improve statistics. In the past, several approaches have been made to parallelize parts of the Monte Carlo algorithm [54–56]. However, most are not practical anymore due to an increase in the performance of single CPUs. If back-polarization is neglected, the electric field can be approximated by the electric field created by static partial charges. The computation of the electric field caused by static partial charges is straightforward [57]. The electric field does not depend on the induced dipoles, and hence no iterative procedure is necessary. Due to this assumption, the change in induction energy solely depends on the induced dipoles of the interaction sites i of the molecule that is involved in the Monte Carlo trial move. The induction energy of a molecule created by the static electric field follows from:

$$U_{\text{ind}} = -\frac{1}{2}\sum_{i=1}^{n} \alpha_i \cdot |\mathbf{E}_i^0|^2, \tag{10}$$

where n is the number of interaction sites belonging to the molecule involved in the Monte Carlo trial move. With Eq. (10), the difference in the induction energy between the old and new configuration of the displaced molecule can be evaluated. To include induction interactions, this energy difference has to be considered in the acceptance rule of the Monte Carlo trial move additional to the changes in energy due to other contributions, e.g., repulsion and dispersion interactions. Lachet et al. [25] showed that the error introduced by the assumption of an static electric field is relatively small. Back-polarization contributes only 6% of the total induction energy in their system. In addition, the contribution of higher order polarizabilities is estimated to be less than 5% of the total induction energy.

For the calculation of the induction energy, atomic polarizabilities α_i are required. In literature, many different sets of polarizabilities are available [58,25,41,59]. However, depending on experimental procedure or theoretical assumption the values of polarizabilities can differ significantly [60]. In addition, the local chemical environment affects the polarization behavior and consequently the polarizability of a molecule [61,62]. Usually, empirical scaling factors are applied to consider differences between gas and condensed phases, whereby different scaling factors are suitable for different classes of molecules [63]. The determination of particular scaling factors often relies on a fitting procedure [64]. To achieve reasonable energies and CO_2 uptakes in the conducted simulations, we apply a global factor to scale all atomic polarizabilities. The initial values of the atomic polarizabilities are taken from the work of van Duijnen and Swart, and Shannon [58,59], which provides a large collection of polarizabilities for atoms and molecules. By fitting to the experimentally determined Henry coefficient of CO_2 in MgMOF-74, we determine the scaling factor in our simulation to 0.09. The adjusted atomic polarizabilities have values of the same magnitude as the ones applied in the simulations of NaY zeolite by Lachet et al. [25].

To account for previously not explicitly incorporated polarization, it is necessary to also adjust the Lennard–Jones interaction parameters that are developed without explicit polarization (and hence contain averaged polarization which needs to be removed) [27]. In our simulations, polarization is only considered between the framework of MgMOF-74 and the adsorbed CO_2 molecules, thus CO_2–CO_2 interaction parameters are not modified. Framework–CO_2 interaction parameters are calculated via the Lorentz–Berthelot mixing rule from the atomic parameters. We use a simple approach to rescale the Lennard–Jones energy parameters for the interactions between CO_2 and the framework with respect to the assigned atomic polarizabilities. The original parameters for MgMOF-74 are taken from the UFF force field [28] and the ones for CO_2 are taken from the TraPPE force field [30]. The Lennard–Jones energy parameter of atom i is adjusted according to:

$$\varepsilon_i^{\text{scaled}} = \varepsilon_i \cdot \frac{(1+\lambda) - \frac{\alpha_i}{\alpha_{\max}}}{(1+\lambda) - \frac{\alpha_i}{\alpha_{\max}} \cdot \lambda}, \tag{11}$$

where λ is a scaling parameter between 0 and 1, and α_i and $\alpha_{\max}$ are the individual and the largest atomic polarizabilities, respectively. The procedure assures that the Lennard–Jones energy parameter ε_i is reduced the most for the atom with the largest atomic polarizability and is unchanged if the atom is not polarizable ($\alpha_i = 0$). By comparing our simulation results to experimental data, we determined λ to be 0.7 ($\alpha_{\max} = 1.591$ which corresponds to the

Fig. 1. Schematic description of the procedure of Lachet et al. [25] to include the induced point dipole method in a Monte Carlo simulation. In our implementation, the electrostatic energy is computed via the Ewald summation technique and the Lennard–Jones potential is truncated at 12.8 Å. No tail correction is applied. For insertions and deletions of molecules in a grand-canonical ensemble the procedure is similar and the acceptance rules are listed in Ref. [32].

Table 1
Scaled Lennard–Jones force field parameters and scaled atomic polarizabilities for MgMOF-74 and CO_2. The original parameters for MgMOF-74 were taken from the UFF force field [28] and the ones for CO_2 are taken from the TraPPE force field [30]. The parameters describing the interactions between framework and adsorbate are adjusted according to Eq. (11). Adsorbate–adsorbate interactions are according to the TraPPE force field (*). The atomic polarizabilities are taken from van Duijnen and Swart, and Shannon [58,59] and scaled with a factor of 0.09. Polarization is only considered between the framework and adsorbate. All molecules are considered to be rigid.

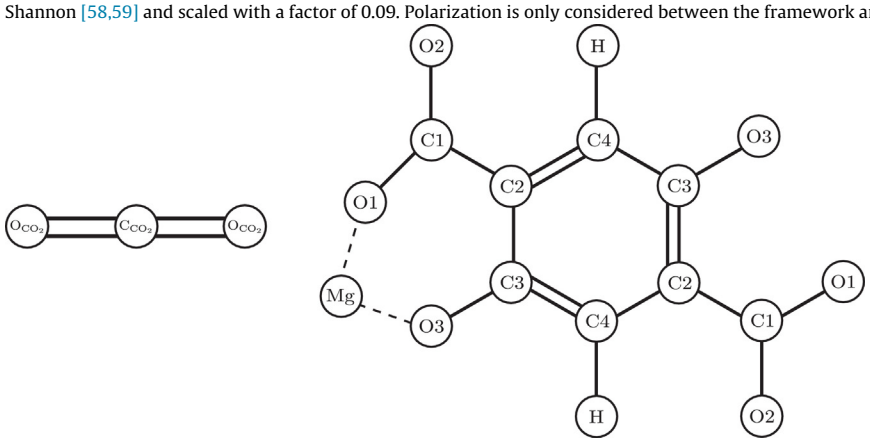

#	Atom type	ε/k_B (K)	σ (Å)	α (Å^3)	Partial charge (e)
1	Mg	55.09	2.69	0.119	1.560
2	O1	27.93	3.12	0.575	−0.899
3	O2	27.93	3.12	0.575	−0.752
4	O3	27.93	3.12	0.575	−0.903
5	C1	45.80	3.43	0.916	0.900
6	C2	45.80	3.43	0.916	−0.314
7	C3	45.80	3.43	0.916	0.456
8	C4	45.80	3.43	0.916	−0.234
9	H	21.30	2.57	0.315	0.186
10	C_{CO_2}	23.40 (27.0*)	2.80	0.916 (−*)	0.700
11	O_{CO_2}	73.08 (79.0*)	3.05	0.575 (−*)	−0.350

polarizability of methane). All force field parameters are summarized in Table 1.

4. Results and discussion

The chosen procedure to scale the atomic polarizabilities and to adjust the Lennard–Jones energy parameters is divided into two steps. In the first step, Widom test particle insertions are conducted to compute the Henry coefficient of CO_2 in MgMOF-74 in the limit of infinite dilution condition [65]. These calculations are computationally relatively cheap. The scaling factor for atomic polarizabilities is adjusted until the predicted Henry coefficient is close to the experimental results. Polarization is of special importance for the low uptake region, where the CO_2 uptake is dominated by the adsorption close to the open metal sites and polarization contributes significantly. These adsorption sites are shown schematically in Fig. 2. The open squares in Fig. 3 represent the adsorption isotherm computed with scaled atomic polarizabilities. While in the low pressure region adsorption is already well predicted, the CO_2 uptake in the relatively high pressure region (i.e., larger than 10^4 Pa) is overestimated. Nevertheless, the overall shape of the adsorption isotherm is in good agreement with experimental measurements. In a second step, the Lennard–Jones energy parameters are adjusted according to Eq. (11). Fig. 3 shows that this particularly improves the simulation results for intermediate to higher pressures. The low pressure region of the adsorption isotherm is affected only slightly, because of the higher relative contribution of the polarization energy.

To better quantify our polarizable force field for the description of interaction energies between adsorbed CO_2 molecules and the framework of MgMOF-74, we compare interaction energies of random CO_2 configurations obtained from DFT calculations with those calculated using the developed polarizable force field. This procedure was previously used by Lin et al. [15] to evaluate the quality of force fields. In Fig. 4(a), the comparison of the polarizable force field and the UFF force field is shown. The polarizable force field describes the interaction energies quite adequately, whereas the UFF force field significantly underestimates the interaction energies for a number of configurations, in particular for those with favorable adsorption energies. Fig. 4(b) shows the interaction energies of the polarizable force field and the previously proposed non-polarizable force field derived from DFT calculations (in this work, we compare our results to model 3 from Lin et al. [15]). In the work of Lin et al., the Buckingham poten-

tial and electrostatic interactions with static partial charges are used without explicitly accounting for polarization. Both force fields model the interaction energies satisfactorily. However, the DFT-derived non-polarizable force field tends to slightly overestimate the interaction energies (i.e., energetically less favorable region with DFT-computed energies larger than −10 kJ/mol) while the polarizable force field shows the opposite trend. On average and considering only those configurations with interaction energies less than 0 kJ/mol in DFT calculations, the absolute differences between force field-based and DFT-based interaction energies are 2.290 kJ/mol, 1.673 kJ/mol and 1.537 kJ/mol for the UFF force field, the polarizable force field and the DFT-derived non-polarizable force field, respectively. Another approach to quantify the differences is the Boltzmann-weighted mean deviation (BMD) [15] defined by:

$$\mathrm{BMD} = \frac{\sum_{j=1}^{N_s} |E_{\mathrm{FF},j} - E_{\mathrm{DFT},j}| \ \exp\left[-\frac{E_{\mathrm{DFT},j}}{k_\mathrm{B}T}\right]}{\sum_{j=1}^{N_s} \exp\left[-\frac{E_{\mathrm{DFT},j}}{k_\mathrm{B}T}\right]}, \tag{12}$$

where $E_{\mathrm{FF},j}$ and $E_{\mathrm{DFT},j}$ are the total guest–host interaction energies for configuration j predicted with force field or with DFT calculations, respectively. k_B is the Boltzmann constant, and N_s is the total number of sampled configurations. For a chosen temperature T of 300 K, the values of BMD are 21.904 kJ/mol, 4.287 kJ/mol and 2.902 kJ/mol for the UFF force field, the polarizable force field, and the DFT-derived non-polarizable force field, respectively. The predicted adsorption isotherms are shown in Fig. 5. The experimental adsorption isotherm [11] shows an inflection between 10^4 and 10^5 Pa. The UFF force field cannot reproduce this behavior and the CO_2 uptake at low pressures that is of direct relevance for carbon capture is largely underestimated. The DFT-derived non-polarizable force field [15] and the polarizable force field both capture the inflection and show significant improvement in the low pressure region. In this region, the CO_2 uptake predicted with the polarizable force field and the DFT-derived non-polarizable force field (i.e., model 3 of Lin et al. [15]) are both in good agreement with the experimental data of Herm et al. [11]. For higher pressures, all three force fields overestimate the CO_2 uptake compared to the experiments. This overestimation is actually expected, since experimental structures show a certain degree of inaccessibility due to diffusion limitation or defects in the crystal structure [9]. In the limit of high pressures, the guest–host interactions become less important and the adsorption is dominated by the accessible volume for CO_2. The TraPPE force field describes the density per void volume well, because it is designed to reproduce the vapor–liquid equilibria. Therefore, the uptake of CO_2 predicted using these three models converge in the high pressure region.

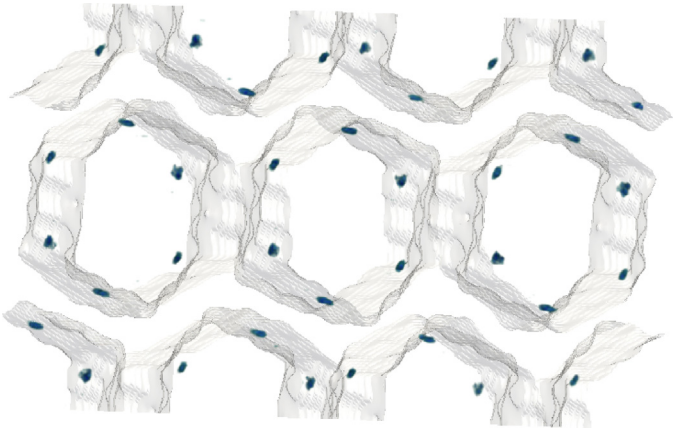

Fig. 2. Graphic representation of the periodic framework of MgMOF-74 with one-dimensional hexagonal channels. The channel surfaces are represented in gray color. The blue-green areas show the most favorable adsorption sites of CO_2 which are close to the open metal sites. (For interpretation of the references to color in this figure legend, the reader is referred to the web version of the article.)

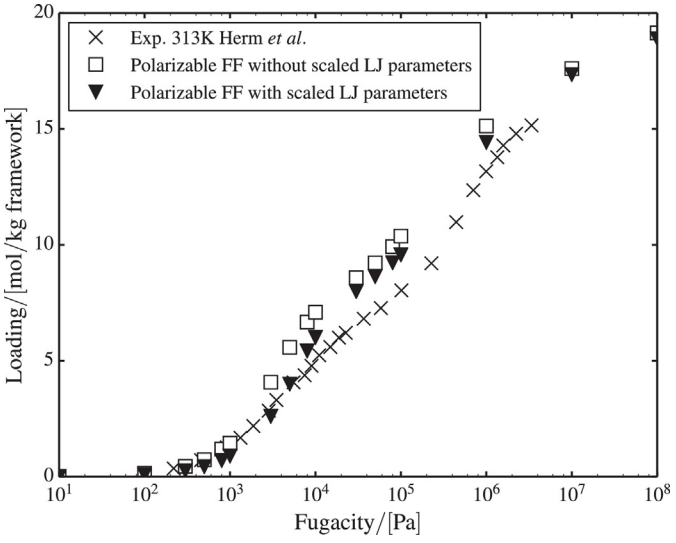

Fig. 3. Comparison between the experimental adsorption isotherm of CO_2 in MgMOF-74 from Herm et al. [11] and the simulated ones using polarizable force fields at 313 K. In both simulations, the atomic polarizabilities are taken from van Duijnen and Swart, and Shannon [58,59] and scaled with a factor of 0.09. The open squares represent the simulation results using the non-scaled Lennard–Jones potential. The adsorption isotherm shown by closed triangles is calculated with a scaling factor λ = 0.7 for the Lennard–Jones potential. In case of the adjusted Lennard–Jones parameters, the simulation results are in much better agreement with the experiments.

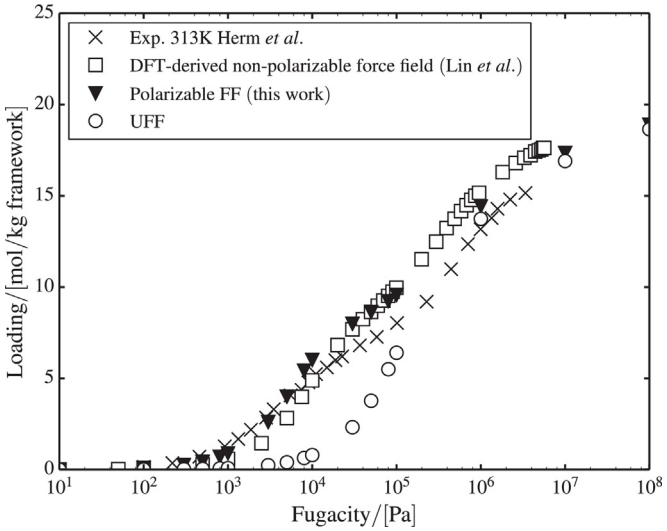

Fig. 5. Comparison between the experimental adsorption isotherm of CO_2 in MgMOF-74 from Herm et al. [11] and the ones predicted from molecular simulations at 313 K. The UFF force field [28] cannot reproduce the inflection of the adsorption isotherm and the CO_2 uptake in the low pressures region. The force field previously developed by Lin et al. (model 3) [15] derived from DFT calculations can capture the adsorption behavior. The simulations conducted with polarizable force field are in good agreement with the experimental results. The low pressure region and the inflection of the adsorption isotherm are well modeled. The used scaling factor λ for the Lennard–Jones potential is 0.7. The atomic polarizabilities are from van Duijnen and Swart, and Shannon [58,59] and scaled with a factor of 0.09.

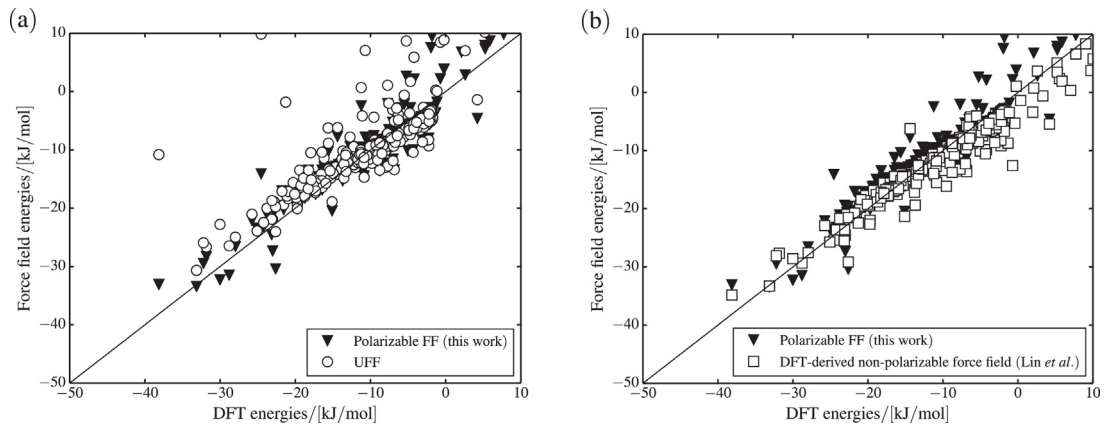

Fig. 4. CO_2–framework interaction energies for a set of 600 randomly located CO_2 configurations in the accessible volume of MgMOF-74. The interaction energies computed in DFT calculations are from Lin et al. (model 3) [15]. The solid line indicates perfect agreement between the force field and DFT energies. (a) Comparison between the polarizable force field and the UFF force field [28]. (b) Comparison between the polarizable force field and the DFT-derived non-polarizable force field [15].

5. Conclusions

With the developed polarizable force field, the adsorption behavior of CO_2 in MgMOF-74 can be accurately described using molecular simulations. The consideration of polarization results in a force field correctly reproducing the inflection of the adsorption isotherm and the CO_2 uptake at the low pressure region. The quality of the predictions is comparable to a previously DFT-derived non-polarizable force field. The straightforward procedure to adjust the atomic polarizabilities and to subsequently re-adjust the Lennard–Jones energy parameters should also be applicable in the evaluation of other MOFs with open metal site for a number of gas separation applications, e.g., carbon capture. Moreover, the consideration of explicit polarization in molecular simulations will result in improved physical models, which provide opportunities for better transferability. We motivated the need to re-adjust the Lennard–Jones energy parameters that were developed to implicitly account for polarization. A promising aim for the future is the development of a DFT-derived force field that explicitly considers polarization. This approach could result in a fully predictive model with excellent transferability of atomic force field parameters. Such a force field would be of great interest for all systems in which polarization has a significant contribution.

Acknowledgments

This work was sponsored by NWO Exacte Wetenschappen (Physical Science) for the use of supercomputer facilities, with financial support from the Nederlandse Organisatie voor Wetenschappelijk Onderzoek (Netherlands Organization for Scientific Research).

References

[1] S. Chu, Carbon capture and sequestration, Science 325 (2009) 1599.
[2] L.-C. Lin, A.H. Berger, R.L. Martin, J. Kim, J.A. Swisher, K. Jariwala, C.H. Rycroft, A.S. Bhown, M.W. Deem, M. Haranczyk, et al., In silico screening of carbon-capture materials, Nat. Mater. 11 (2012) 633–641.
[3] R.S. Haszeldine, Carbon capture and storage: how green can black be? Science 325 (2009) 1647–1652.
[4] B. Smit, J.R. Reimer, C.M. Oldenburg, I.C. Bourg, Introduction to Carbon Capture and Sequestration, Imperial College Press, London, 2014.
[5] J.M. Huck, L.-C. Lin, A.H. Berger, M.N. Shahrak, R.L. Martin, A.S. Bhown, M. Haranczyk, K. Reuter, B. Smit, Evaluating different classes of porous materials for carbon capture, Energy Environ. Sci. 7 (2014) 4132–4146.
[6] C.E. Wilmer, M. Leaf, C.Y. Lee, O.K. Farha, B.G. Hauser, J.T. Hupp, R.Q. Snurr, Large-scale screening of hypothetical metal-organic frameworks, Nat. Chem. 4 (2012) 83–89.
[7] T.F. Willems, C.H. Rycroft, M. Kazi, J.C. Meza, M. Haranczyk, Algorithms and tools for high-throughput geometry-based analysis of crystalline porous materials, Microporous Mesoporous Mater. 149 (2012) 134–141.
[8] J.A. Mason, K. Sumida, Z.R. Herm, R. Krishna, J.R. Long, Evaluating metal-organic frameworks for post-combustion carbon dioxide capture via temperature swing adsorption, Energy Environ. Sci. 4 (2011) 3030–3040.
[9] P.D.C. Dietzel, V. Besikiotis, R. Blom, Application of metal-organic frameworks with coordinatively unsaturated metal sites in storage and separation of methane and carbon dioxide, J. Mater. Chem. 19 (2009) 7362–7370.
[10] W.L. Queen, C.M. Brown, D.K. Britt, P. Zajdel, M.R. Hudson, O.M. Yaghi, Site-specific CO_2 adsorption and zero thermal expansion in an anisotropic pore network, J. Phys. Chem. C 115 (2011) 24915–24919.
[11] Z.R. Herm, J.A. Swisher, B. Smit, R. Krishna, J.R. Long, Metal-organic frameworks as adsorbents for hydrogen purification and precombustion carbon dioxide capture, J. Am. Chem. Soc. 133 (2011) 5664–5667.
[12] A. Yazaydin, R.Q. Snurr, T.-H. Park, K. Koh, J. Liu, M.D. LeVan, A.I. Benin, P. Jakubczak, M. Lanuza, D.B. Galloway, J.J. Low, R.R. Willis, Screening of metal-organic frameworks for carbon dioxide capture from flue gas using a combined experimental and modeling approach, J. Am. Chem. Soc. 131 (2009) 18198–18199.
[13] R. Krishna, J.M. van Baten, Investigating the potential of MgMOF-74 membranes for CO_2 capture, J. Membr. Sci. 377 (2011) 249–260.
[14] A.L. Dzubak, L.-C. Lin, J. Kim, J.A. Swisher, R. Poloni, S.N. Maximoff, B. Smit, L. Gagliardi, Ab initio carbon capture in open-site metal-organic frameworks, Nat. Chem. 4 (2012) 810–816.
[15] L.-C. Lin, K. Lee, L. Gagliardi, J.B. Neaton, B. Smit, Force-field development from electronic structure calculations with periodic boundary conditions: applications to gaseous adsorption and transport in metalorganic frameworks, J. Chem. Theory Comput. 10 (2014) 1477–1488.
[16] L. Chen, C.A. Morrison, T. Düren, Improving predictions of gas adsorption in metal-organic frameworks with coordinatively unsaturated metal sites: model potentials, ab initio parameterization, and GCMC simulations, J. Phys. Chem. C 116 (2012) 18899–18909.
[17] H. Wu, J.M. Simmons, G. Srinivas, W. Zhou, T. Yildirim, Adsorption sites and binding nature of CO_2 in prototypical metal-organic frameworks: a combined neutron diffraction and first-principles study, J. Phys. Chem. Lett. 1 (2010) 1946–1951.
[18] D. Dubbeldam, K.S. Walton, On the application of classical molecular simulations of adsorption in metal-organic frameworks, in: J. Jiang (Ed.), Metal-Organic Frameworks: Materials Modeling Towards Engineering Applications, Pan Stanford, Singapore, 2015, pp. 53–112.
[19] H.S. Antila, E. Salonen, Polarizable force fields, in: L. Monticelli, E. Salonen (Eds.), Biomolecular Simulations, Humana Press, New York City, 2013, pp. 215–241.
[20] S.W. Rick, S.J. Stuart, Potentials and Algorithms for Incorporating Polarizability in computer simulations, in: K.B. Lipkowitz, D.B. Boyd (Eds.), in: Reviews in Computational Chemistry, vol. 18, John Wiley & Sons, Inc., Hoboken, 2003, pp. 89–146.
[21] T.A. Halgren, W. Damm, Polarizable force fields, Curr. Opin. Struct. Biol. 11 (2001) 236–242.
[22] M.G. Martin, B. Chen, J.I. Siepmann, A novel Monte Carlo algorithm for polarizable force fields: application to a fluctuating charge model for water, J. Chem. Phys. 108 (1998) 3383–3385.
[23] P. Cieplak, J. Caldwell, P. Kollman, Molecular mechanical models for organic and biological systems going beyond the atom centered two body additive approximation: aqueous solution free energies of methanol and N-methyl acetamide, nucleic acid base, and amide hydrogen bonding and chloroform/water partition coefficients of the nucleic acid bases, J. Comput. Chem. 22 (2001) 1048–1057.

[24] P. Cieplak, P. Kollman, Monte Carlo simulation of aqueous solutions of Li^+ and Na^+ using manybody potentials. Coordination numbers, ion solvation enthalpies, and the relative free energy of solvation, J. Chem. Phys. 92 (1990) 6761–6767.
[25] V. Lachet, A. Boutin, B. Tavitian, A.H. Fuchs, Computational study of p-xylene/m-xylene mixtures adsorbed in NaY zeolite, J. Phys. Chem. B 102 (1998) 9224–9233.
[26] A.J. Stone, The Theory of Intermolecular Forces, International Series of Monographs on Chemistry ed., Clarendon Press, Oxford, 1996.
[27] A.J. Stone, Intermolecular potentials, Science 321 (2008) 787–789.
[28] A.K. Rappe, C.J. Casewit, K.S. Colwell, W.A. Goddard, W.M. Skiff, UFF, a full periodic table force field for molecular mechanics and molecular dynamics simulations, J. Am. Chem. Soc. 114 (1992) 10024–10035.
[29] S.L. Mayo, B.D. Olafson, W.A. Goddard, Dreiding: a generic force field for molecular simulations, J. Phys. Chem. 94 (1990) 8897–8909.
[30] J.J. Potoff, J.I. Siepmann, Vapor–liquid equilibria of mixtures containing alkanes, carbon dioxide, and nitrogen, AIChE J. 47 (2001) 1676–1682.
[31] J.N. Israelachvili, Repulsive steric forces, total intermolecular pair potentials, and liquid structure, in: Intermolecular and Surface Forces, third ed., Academic Press, San Diego, 2011, pp. 133–149.
[32] D. Frenkel, B. Smit, Understanding Molecular Simulation, second ed., Academic Press, San Diego, 2002.
[33] T. Darden, D. York, L. Pedersen, Particle Mesh Ewald: an Nlog(N) method for Ewald sums in large systems, J. Chem. Phys. 98 (1993) 10089–10092.
[34] D. Wolf, P. Keblinski, S.R. Phillpot, J. Eggebrecht, Exact method for the simulation of Coulombic systems by spherically truncated, pairwise r^{-1} summation, J. Chem. Phys. 110 (1999) 8254–8282.
[35] C.J. Fennell, J.D. Gezelter, Is the Ewald summation still necessary? Pairwise alternatives to the accepted standard for long-range electrostatics, J. Chem. Phys. 124 (2006) 234104.
[36] N.D. Spencer, J.H. Moore, Encyclopedia of Chemical Physics and Physical Chemistry: Applications, Third Volume, Taylor & Francis, 2001.
[37] J.N. Israelachvili, Van der Waals Forces, in: Intermolecular and Surface Forces, third ed., Academic Press, San Diego, 2011, pp. 107–132.
[38] M.D. LeVan, G. Carta, C.M. Yon, Adsorption and ion exchange, in: R.H. Perry, D.W. Green (Eds.), Perry's Chemical Engineers' Handbook, seventh ed., McGraw-Hill, New York, 1997, pp. 11–16.
[39] P. Atkins, J. de Paula, Molecular Interactions, Atkins' Physical Chemistry, eighth ed., W. H. Freeman and Company, New York, 2006, pp. 620–651.
[40] X. He, L. Fusti-Molnar, G. Cui, K.M. Merz Jr., Intermolecular potential function for the physical adsorption of rare gases in silicalite, J. Phys. Chem. B 113 (2009) 5290–5300.
[41] R.J.-M. Pellenq, D. Nicholson, Importance of dispersion and electron correlation in ab initio protein folding, J. Phys. Chem. 98 (1994) 13339–13349.
[42] T. van Westen, T.J.H. Vlugt, J. Gross, Determining force field parameters using a physically based equation of state, J. Phys. Chem. B 115 (2011) 7872–7880.
[43] C.S. Schacht, T.J.H. Vlugt, J. Gross, Using an analytic equation of state to obtain quantitative solubilities of CO_2 by molecular simulation, J. Phys. Chem. Lett. 2 (2011) 393–396.
[44] G. Kresse, J. Hafner, Ab initio molecular dynamics for liquid metals, Phys. Rev. B 47 (1993) 558.
[45] S.T. Russell, A. Warshel, Calculations of electrostatic energies in proteins: the energetics of ionized groups in bovine pancreatic trypsin inhibitor, J. Mol. Biol. 185 (1985) 389–404.
[46] H. Yu, W.F. van Gunsteren, Accounting for polarization in molecular simulation, Comput. Phys. Commun. 172 (2005) 69–85.
[47] A. Warshel, K. Mitsunori, A.V. Pisliakov, Polarizable force fields: history, test cases, and prospects, J. Chem. Theory Comput. 3 (2007) 2034–2045.
[48] P. Cieplak, F.-Y. Dupradeau, Y. Duan, J. Wang, Polarization effects in molecular mechanical force fields, J. Phys.: Condens. Matter 21 (2009) 333102.
[49] P.E.M. Lopes, B. Roux, A.D. MacKerell Jr., Molecular modeling and dynamics studies with explicit inclusion of electronic polarizability: theory and applications, Theor. Chem. Acc. 124 (2009) 11–28.
[50] P.J. Mitchell, D. Fincham, Shell model simulations by adiabatic dynamics, J. Phys.: Condens. Matter 5 (1993) 1031–1038.
[51] D. Dubbeldam, S. Calero, D.E. Ellis, R.Q. Snurr, RASPA: molecular simulation software for adsorption and diffusion in flexible nanoporous materials, Molecular Simulation (2015), http://dx.doi.org/10.1080/08927022.2015.1010082.
[52] D. Dubbeldam, A. Torres-Knoop, K.S. Walton, On the inner workings of Monte Carlo codes, Mol. Simul. 39 (2013) 1253–1292.
[53] T.R.C. Van Assche, T. Duerinck, J.J. Gutirrez Sevillano, S. Calero, G.V. Baron, J.F.M. Denayer, High adsorption capacities and two-step adsorption of polar adsorbates on copperbenzene-1,3,5-tricarboxylate metalorganic framework, J. Phys. Chem. C 117 (2013) 18100–18111.
[54] K. Esselink, L.D.J.C. Loyens, B. Smit, Parallel Monte Carlo simulations, Phys. Rev. E 51 (1995) 1560–1568.
[55] L.D.J.C. Loyens, B. Smit, K. Esselink, Parallel Gibbs-ensemble simulations, Mol. Phys. 86 (1995) 171–183.
[56] T.J.H. Vlugt, Efficiency of parallel CBMC simulations, Mol. Simul. 23 (1999) 63–78.
[57] T.M. Nymand, P. Linse, Ewald summation and reaction field methods for potentials with atomic charges, dipoles, and polarizabilities, J. Chem. Phys. 112 (2000) 6152–6160.
[58] P.T. van Duijnen, M. Swart, Molecular and atomic polarizabilities: Thole's model revisited, J. Phys. Chem. A 102 (1998) 2399–2407.
[59] R.D. Shannon, Dielectric polarizabilities of ions in oxides and fluorides, J. Appl. Phys. 73 (1993) 349–366.
[60] K.D. Bonin, V.V. Kresin, Electric-dipole polarizabilities of atoms, molecules, and clusters, World Scientific, Singapore, 1997.
[61] Y. Tu, A. Laaksonen, The electronic properties of water molecules in water clusters and liquid water, Chem. Phys. Lett. 329 (2000) 283–288.
[62] M. In Het Panhuis, P.L.A. Popelier, R.W. Munn, J.G. Ángyán, Distributed polarizability of the water dimer: field-induced charge transfer along the hydrogen bond, J. Chem. Phys. 114 (2001) 7951–7961.
[63] C.M. Baker, J.A.D. MacKerell, Polarizability rescaling and atom-based Thole scaling in the CHARMM Drude polarizable force field for ethers, J. Mol. Model. 16 (2010) 567–576.
[64] C.R. Vosmeer, A.S. Rustenburg, J.E. Rice, H.W. Horn, W.C. Swope, D.P. Geerke, QM/MM-based fitting of atomic polarizabilities for use in condensed-phase biomolecular simulation, J. Chem. Theory Comput. 8 (2012) 3839–3853.
[65] T.J.H. Vlugt, E. García-Pérez, D. Dubbeldam, S. Ban, S. Calero, Computing the heat of adsorption using molecular simulations: the effect of strong Coulombic interactions, J. Chem. Theory Comput. (2008) 1107–1118.

Tim M. Becker received his B.Sc. and M.Sc. degree from RWTH Aachen University (Germany). After his graduation in 2014, he moved to Delft University of Technology (The Netherlands) as a Ph.D. student working with Thijs J.H. Vlugt and David Dubbeldam. His research involves the simulation of solid adsorbents.

David Dubbeldam received his B.Sc. and Ph.D. degree (with honors) from the University of Amsterdam (The Netherlands), in Computer Science and Computational Chemistry. From 2006 until 2009, he carried out a postdoctoral stay at Northwestern University (U.S.A.) in the group of Professor Randall Q. Snurr, working on modeling of adsorption and diffusion in flexible metal-organic frameworks. In 2010 he joined the Computational Chemistry Group at the University of Amsterdam as an assistant professor.

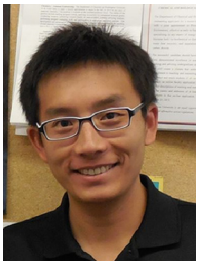

Li-Chiang Lin received his B.Sc. and M.Sc. degree in Chemical Engineering from National Taiwan University (Taiwan). In 2014, he was awarded the Ph.D. degree in Chemical Engineering from the Dept. of Chemical and Biomolecular Engineering at the University of California, Berkeley (U.S.A.). After his doctoral study, he worked at the Massachusetts Institutes of Technology (U.S.A.) as a postdoctoral researcher. In 2015, he joined the Dept. of Process and Energy at Delft University (The Netherlands) as an assistant professor.

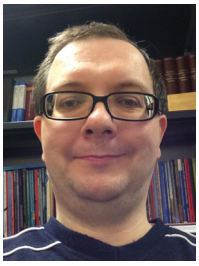

Thijs J.H. Vlugt received his M.Sc. degree in Chemical Engineering in 1997 at Eindhoven University of Technology. In 2000, he obtained his Ph.D. degree at the University of Amsterdam with R. Krishna and Berend Smit as thesis advisors. After postdoctoral research in Mainz (Germany) and Leiden (The Netherlands), he was appointed assistant professor at Utrecht University. In 2007 he moved to Delft University of Technology, first as associate professor and later as full professor and chair Engineering Thermodynamics (2010). In 2005 he received a prestigious VIDI personal grant for research on the self-assembly on nanocrystals. He is also director of the honours program at the faculty of Mechanical, Maritime, and Materials Engineering in Delft. He has co-authored over 170 scientific publications.